
Model Provenance via Model DNA

Xin Mu, Yu Wang, Yehong Zhang, Jiaqi Zhang, Hui Wang, Yang Xiang, Yue Yu
Peng Cheng Laboratory
Shenzhen, China
{mux, wangy12, zhangyh02, zhangjq02, wangh06, xiangy, yuy}@pcl.ac.cn

Abstract

Understanding the life cycle of the machine learning (ML) model is an intriguing area of research (e.g., understanding where the model comes from, how it is trained, and how it is used). This paper focuses on a novel problem within this field, namely Model Provenance (MP), which concerns the relationship between a target model and its pre-training model and aims to determine whether a source model serves as the provenance for a target model. This is an important problem that has significant implications for ensuring the security and intellectual property of machine learning models but has not received much attention in the literature. To fill in this gap, we introduce a novel concept of Model DNA which represents the unique characteristics of a machine learning model. We utilize a data-driven and model-driven representation learning method to encode the model’s training data and input-output information as a compact and comprehensive representation (i.e., DNA) of the model. Using this model DNA, we develop an efficient framework for model provenance identification, which enables us to identify whether a source model is a pre-training model of a target model. We conduct evaluations on both computer vision and natural language processing tasks using various models, datasets, and scenarios to demonstrate the effectiveness of our approach in accurately identifying model provenance.

1 Introduction

In recent years, machine learning has become a ubiquitous presence in various fields, revolutionizing industries ranging from healthcare to finance [Shehab et al., 2022, Dixon et al., 2020]. With the release of OpenAI’s GPT-4, the capabilities of machine learning are poised to reach even greater heights¹. However, as the value of data as an emerging asset class becomes increasingly recognized, the issue of protecting the intellectual property of machine learning models has become a pressing concern [Xue et al., 2021]. Indeed, the machine learning model itself can be viewed as a digital good, further emphasizing the need for robust intellectual property protection measures.

To protect the intellectual property of a machine learning model, it is critical to understand the entire life cycle of the model, e.g., understanding where the model comes from, how it is trained, and how it is used. In this paper, we explore a new and important problem within the research direction of understanding the machine learning model life cycle, namely Model Provenance (MP). This problem aims to investigate the relationship between two models, such as understanding whether a target model is derived from a source model. To illustrate this problem, consider a real-world business scenario in which an AI company seeks to protect the intellectual property of its machine learning model trained on private data using a significant amount of computing power. The company wishes to ensure that the model is only used by authorized users. However, in practice, authorized users may share the model with unauthorized users without the company’s permission, or the model may be stolen and used by an unauthorized user. The unauthorized user may then use the stolen model to

¹<https://openai.com/research/gpt-4>

develop their own products based on techniques such as continual learning [Parisi et al., 2019a]. This situation presents a significant challenge: how can an AI company identify whether a source model, owned by an authorized user, is the provenance of a target model developed by an unauthorized user?

A related study is that discussing the influence of the pre-training model in continual learning or lifelong learning. For example, Mehta et al. [2021] observed that generic pre-training implicitly alleviates the effects of catastrophic forgetting when learning multiple tasks sequentially compared to randomly initialized models. Toneva et al. [2019] showed that catastrophic forgetting is observed in the continual learning setting. Although those existing works discussed the relationship across different tasks within studying the phenomenon of catastrophic forgetting, there is no method for identifying the relationship between different models across different tasks, to the best of our knowledge.

In this paper, we address the problem of model provenance and begin by formalizing this problem and conducting an empirical study to evaluate the performance of the target model on the source model’s training data (Section 3), whose results inspire us to ask whether we can create a description to explain the relationship between the source and target models. Then, we introduce a novel concept of model DNA, which represents the unique characteristics of a machine learning model, and propose a framework for model DNA generation and model provenance identification. The effectiveness of our approach is demonstrated through both Computer Vision (CV) and Natural Language Processing (NLP) tasks.

In this paper, we make three key contributions as follows:

- This paper makes a significant contribution to the field of machine learning model understanding by addressing an important research direction related to the life cycle of ML models, i.e., identifying the relationship between a pre-training model and its downstream models. This problem is crucial for tracking the model evolution and contributing to protecting the intellectual property of the machine learning model.
- We propose a novel machine learning model representation, called Model DNA, which combines data-driven and model-driven approaches to encode the training data and input-output information as a compact and comprehensive representation of the model (Section 4). In DNA space, we can easily measure the similarity between models and track their usage and evolution over time. Based on this idea, we introduce the Model Provenance framework, which includes Model DNA generation and provenance identification, providing a practical solution for identifying relationships between models and better understanding the provenance of machine learning models (Section 5).
- We perform extensive experiments to assess the effectiveness of our proposed framework on various commonly used CV and NLP benchmark datasets along with DNN structure models. To enhance the understanding, we present comprehensive visualizations of the distribution of Model DNA in the DNA space (Section 6).

2 Related work

Lifelong learning. Lifelong machine learning is a learning paradigm that continuously accumulates past knowledge and adapts it to future learning and problem-solving [Lange et al., 2022, Chen and Liu, 2018, Parisi et al., 2019b]. This involves performing a sequence of N learning tasks, $\mathcal{T}_1, \mathcal{T}_2, \dots, \mathcal{T}_N$, each with its corresponding dataset D_1, D_2, \dots, D_N of different types and from different domains. When faced with a new task \mathcal{T}_{N+1} (called the current task) with its data D_{N+1} , the learner can use past knowledge to aid in learning. One of the major challenges in lifelong learning is catastrophic forgetting, where the model forgets previously learned information when learning new tasks. To mitigate this phenomenon, approaches can be categorized into three groups: (1) regularization-based approaches [Kirkpatrick et al., 2017, Zenke et al., 2017], (2) memory-based approaches [Lopez-Paz and Ranzato, 2017, Chaudhry et al., 2019, Wang et al., 2020], and (3) network expansion-based approaches [Rusu et al., 2016, Aljundi et al., 2017, Sodhani et al., 2020]. The focus of this paper is to distinguish the relationship between the model from the previous task and the current task, which is an under-explored direction in existing lifelong learning works.

Representation Learning. Representation learning refers to the process of learning a parametric mapping from the raw input data domain to a feature vector, in the hope of capturing and extracting

more abstract and useful concepts that can improve performance on a range of downstream tasks. The aim of learning representations of the data is to make it easier to extract useful information when building classifiers or other predictors. Representation learning has played a tremendous role in different SOTA frameworks [Bengio et al., 2013]. Recently, Contrastive Representation Learning (CRL) is widely used in NLP and CV [Le-Khac et al., 2020]. It can be considered as self-supervised learning by comparing among different samples [Chen et al., 2020, van den Oord et al., 2018]. In this paper, we explore a way of machine learning model representation. Our approach involves a data-driven and model-driven representation learning framework that constructs a model representation in a latent space. This work is novel since it is the first time, as far as we know, that such an approach is proposed for representing the ML model.

Data Provenance. The area of data provenance is also relevant and falls under the provenance research family. In general, the problem is defined by auditing if a certain piece of data has been used to train a machine learning model [Song and Shmatikov, 2019, Mu et al., 2022, Maini et al., 2021]. It is also called *membership inference attacks* [Shokri et al., 2017, Hu et al., 2021]. A data provenance technique (i.e., shadow training) has been widely studied, which can successfully audit deep learning-based models [Shokri et al., 2017, Song and Shmatikov, 2019]. The main idea is to use multiple shadow models to imitate the behavior of the target model. As the training data for the shadow models are known, the target model can be trained using the labeled outputs of the shadow models. However, this is a data-level provenance problem, whereas our focus is on the model-level provenance problem.

3 Model Provenance (MP): Definition

Consider a dataset $D_s = \{(x_i, y_i)\}_{i=1}^{|D_s|}$ where each $x_i \in \mathbb{R}^d$ is a data instance and $y_i \in Y = \{1, 2, \dots, c\}$ is its associated class label. Using an algorithm architecture \mathcal{A}_s , a machine learning model M_s is learned from D_s . Let $D_t = (x_j, y_j)_{j=1}^{|D_t|}$ be a dataset used to learn another machine learning model M_t . If M_t is learned using the pre-training model M_s with the same algorithm architecture \mathcal{A}_s , we refer to M_s as the source model and M_t as the homologous model of M_s . Similarly, let \bar{M}_t be a machine learning model learned from the dataset $D_t = (x_j, y_j)_{j=1}^{|D_t|}$ but based on random initialization or pre-training without using M_s . We refer \bar{M}_t as non-homologous to M_s .

The problem of *Model Provenance (MP)* is to find a function f such that for a given source model M_s and any target model M_1 ,

$$f(M_s, M_1) = \begin{cases} 1, & \text{if } M_1 \text{ is the homologous model of } M_s. \\ 0, & \text{otherwise.} \end{cases} \quad (1)$$

When $f(M_s, M_1) = 1$, we also say M_s is the provenance of M_1 .

The MP problem can have various variations, depending on the conditions imposed on the target model M_t . For instance, a hard condition is when M_t is trained based on sub-parameters of pre-training model M_s , or when the structure of M_t is adjusted to be different from that of M_s . A relaxation of this condition is when the structure of M_t is the same as that of M_s and the training is entirely based on the pre-training model M_s . In this paper, we mainly focus on MP under the relaxation condition. The MP of more complex models under the hard condition will be considered in our future work. In addition, the focus of this paper is on the process of model provenance taking place on the source model owner’s side. We assume that the training dataset of the source model can be accessed for this task.

Discussion. In the field of continual learning, there have been several studies focused on quantifying the relationship between homologous models, such as the analysis of catastrophic forgetting [Mirzadeh et al., 2020, Keskar et al., 2017, Mehta et al., 2021]. For example, Mirzadeh et al. [2020] provided a theoretical bound on forgetting in sequential learning. Let $L(w)$ be the loss on the training dataset with model parameter w , and w_1 and w_2 be the optimal or convergent parameters after training the source and homologous models sequentially. Specifically, they showed that

$$L_1(w_2) - L_1(w_1) \approx \frac{1}{2} \Delta w^\top \nabla^2 L_1(w_1) \Delta w \leq \frac{1}{2} \lambda_1^{max} \|\Delta w\| \quad (2)$$

where $L_1(w_1)$ and $L_1(w_2)$, respectively, represent the losses on source training dataset with parameters w_1 and w_2 , $\Delta w = w_2 - w_1$, and λ_1^{max} is the largest eigenvalue of the Hessian matrix $\nabla^2 L_1(w_1)$.

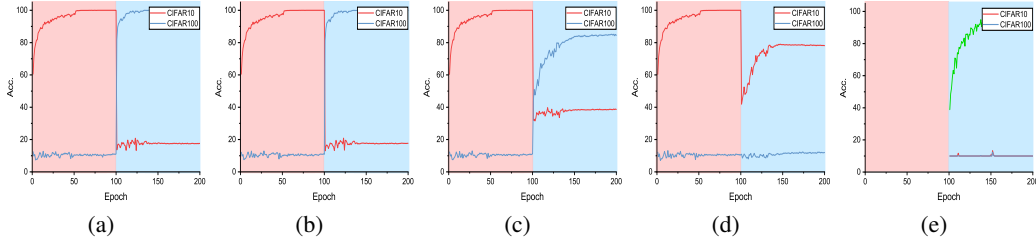


Figure 1: Resnet18. (a) No replace layer. (b) Replace target model’s last layer with source model. (c) Replace last two layers. (d) Replace last three layers. (e) Replace target model (random initialization)’s last three layers with source model.

The eigenvalues of the Hessian matrix are indicative of the curvature of the loss function [Keskar et al., 2017], where smaller eigenvalues imply a flatter loss function. Thus, λ_1^{max} is considered as a proxy for the flatness of the loss function (lower is flatter). Meanwhile, empirical studies conducted by Mehta et al. [2021] and Mirzadeh et al. [2020] show that initializing models with pre-trained weights results in a relatively flat task minima, and flatter models tend to have smaller Δw than less flat ones.

These existing works have motivated us to a straightforward solution for model provenance, i.e., using the difference of Δw to distinguish between homologous and non-homologous models. We can expect that $\Delta w = w_2 - w_1$ would be smaller for homologous models compared to non-homologous models based on the above analysis. However, we found that this solution did not work well in practice. The main issue was that it is impossible to know how flat the target model is, which makes it difficult to use the difference of Δw as a reliable indicator of model provenance.

Furthermore, we conducted experiments using the standard continual learning setup on image classification tasks [Toneva et al., 2019, Paul et al., 2021] to show the relationship between homologous models. Specifically, we examined two model architectures, ResNet18 [He et al., 2016] and AlexNet [Krizhevsky et al., 2012], on the CIFAR10 and CIFAR100 datasets. A source model M_s is first trained on CIFAR10. Then we randomly select ten classes from CIFAR100 to train target models M_t . Note that M_t is learned by initializing its parameters using those of the source model M_s . In Figure 1, we present the results of the experiments conducted on ResNet18. The results for AlexNet are similar and can be found in the supplementary material. The background color indicates the different training phases. The red color represents the training of source model M_s on the CIFAR10 dataset, while the blue color represents the training of target model M_t on the CIFAR100 dataset. The red line corresponds to the accuracy of testing the model on the training data of CIFAR10, while the blue line represents the accuracy of testing the model on the training data of CIFAR100. In the blue background part, we train the model based on the parameters of the model obtained in the red background part.

Figure 1 (a) demonstrates that the predictive accuracy of M_t is significantly reduced when evaluated on the CIFAR10 dataset (as shown by the red line in the blue section). This observation suggests that the training data of the source model may have been severely forgotten in the homologous model (i.e., large $\|\Delta w\|$). Figures 1 (b)-(d) provide further insight into the relationship between the source model M_s and the homologous model M_t . They show the predictive accuracy of M_t on the CIFAR10 dataset when different number of last layers of M_t are replaced with corresponding layers in M_s . We can observe that as we replace more layers in M_t with those from M_s , the predictive accuracy of M_t on the CIFAR10 dataset increases. To investigate this further, we also conducted an experiment with \bar{M}_t being randomly initialized and its last layers replaced with those from M_s . Figure 1 (e) shows that even with the last layers replaced, the predictive accuracy of \bar{M}_t is still poor. The green line in Figure 1 (e) represents the training accuracy of \bar{M}_t .

Overall, our discussion has demonstrated the existence of a relationship between the source model and its homologous model, as shown by the improvement in predictive accuracy when replacing the last layers of the target model with those of the source model. These results led us to pose the question: "Can we establish a relationship between a source model and its homologous or non-homologous model based on the training data of the source model?" and motivated us to introduce the Model DNA and Model Provenance framework, which we present in the following sections.

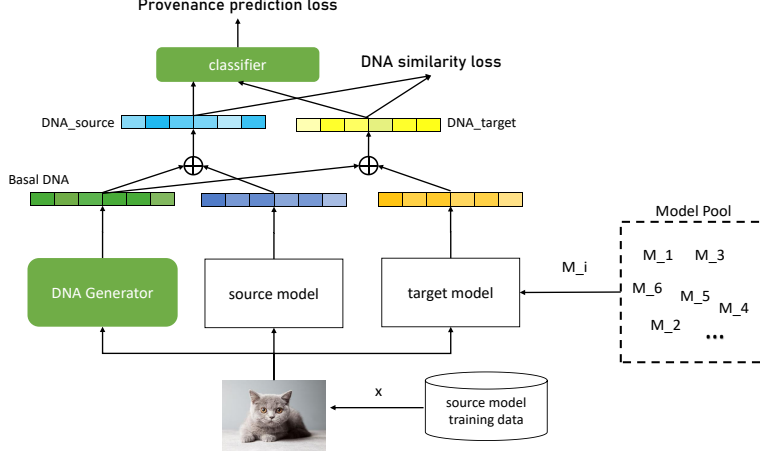


Figure 2: The MGMP framework

4 What is model DNA?

Generally, deoxyribonucleic acid (abbreviated DNA) represents the molecule that carries the genetic information for the development and functioning of an organism in the biology field [Ridley, 2000]. For the Machine Learning (ML) community, we define the model DNA as a kind of representation of a ML model. Like previous studies of representation learning [Bengio et al., 2013], the representation of the model can help us with distinguishing the discrepancy between different model versions across various tasks and can be used to compare and measure the similarity between different models.

As we know, an ML model is generally trained from a dataset D and an algorithm architecture \mathcal{A}_s . Therefore, we consider the DNA generation which has taken into account both the influence of the dataset D and the input-output relation of the model. We define the model DNA as follows:

Definition 1 (Model DNA): Let D be a set of N training data of a machine learning model M . We define the model DNA as a set of N DNA fragment $\mathbb{O} = \{o_1, o_2, \dots, o_N\}$, where each DNA fragment o_i is corresponding to a training sample of the model. It can be generated as $\mathbb{O} \leftarrow g(D, M)$ where $g(\cdot)$ is an approach for DNA generation. A DNA fragment o_i is generated by $g(x_i, M)$ for $x_i \in D$.

By modeling model DNA, we construct a latent space of the model representation that has all different ML models' DNA. In this space, we can leverage or measure the relationship between different ML models. In this paper, we assume DNA fragment o_i is a vector that is generated by $o_i \leftarrow g(x_i, M), x_i \in D$. Notice that in general, we assume the DNA of the homologous models is closer and the non-homologous models are further apart. This latent space leads to the following properties of model DNA described below.

Let \mathbb{O}_i be the model DNA of any model M_i and \mathbb{D} represent the distance function such that $\mathbb{D}(o_i^s, o_j^t)$ is the distance between DNA fragments of any two models M_s and M_t . The following properties of DNA latent space are desired:

- Different ML models have different DNA: If $M_s \neq M_t, \mathbb{O}_s \neq \mathbb{O}_t$.
- The homologous models should have similar DNA fragments and vice versa: $\mathbb{D}(o_i^s, o_i^t) < \mathbb{D}(o_i^s, \bar{o}_i^t)$, where $o_i^s \leftarrow g(x_i, M_s), o_i^t \leftarrow g(x_i, M_t)$ and $\bar{o}_i^t \leftarrow g(x_i, \bar{M}_t)$. M_t is trained based on the pre-training model M_s , whereas \bar{M}_t is trained without using M_s .
- The DNA fragments from the same ML model should be similar: $\forall i, j, i \neq j, \mathbb{D}(o_i, o_j)$ should be minimized for $o_i, o_j \in \mathbb{O}$.

In the following, we introduce our proposed framework for addressing the MP problem, which carefully designs a mechanism to satisfy the aforementioned model DNA properties. Our framework considers both the source model's training data and the input-output relationship of the model to generate a model DNA. We provide more details on this mechanism in the next section.

5 The proposed framework

We propose a framework with Model DNA Generation and the Model Provenance identification (**MGMP**) based on deep representation learning. The main idea behind **MGMP** is to use the intrinsic features of a machine learning model and its training data to generate a model representation using deep neural networks. This model representation, referred to as the model DNA, is a vector that encodes the input-output properties of the model and its training data. The proposed model comprises three major components: the DNA generation, DNA similarity loss, and provenance classifier, which are illustrated in Figure 2. The input to **MGMP** is the training data of the source model, which is then passed to the DNA generator along with the source and target model. We compute the outputs of DNA generator, source model, and target model. The results are combined to produce model DNA, e.g., combining results of the DNA generator and model outputs. After that, we achieve the model DNA of the source model and target model. A DNA similarity loss is employed to preserve the information between homologous and non-homologous models. Finally, the model DNA is used to train a dichotomous outcome prediction network to obtain provenance outcomes. Next, we describe each component of **MGMP** in detail.

5.1 DNA generation

DNA generation is a data-driven and model-driven process of learning representation of a machine learning model. Inspired by Goodfellow et al. [2020], we begin by initializing a generator $g(\cdot)$ using a standard deep neural network (it is important to note that the generator can be constructed using any complex deep generative model). The generator has multiple hidden layers and uses the rectified linear unit (ReLU) activation function. Given an input data point x_i , we generate a latent representation $z_i = g(x_i)$, where $g(\cdot)$ represents the learned DNA generation function implemented by the deep network. The **MGMP** framework utilizes the training data D_s of the source model as its own training data. Specifically, we feed each training data point x_i to the DNA generator, source model, and target model separately, as follows:

$$z_i \leftarrow g(x_i), \quad y_i^s \leftarrow M_s(x_i), \quad y_i^t \leftarrow M_t(x_i). \quad (3)$$

Model pool. The aim of the proposed framework is to establish a common representation space that facilitates the comparison of different models, including both homologous and non-homologous ones. To achieve this, we employ a model pool that consists of various models that exhibit different relationships with the source model. In each mini-batch, we select a pair of models (M_t, \bar{M}_t) to represent the target model (as shown in Figure 2), where M_t is learned based on the source model M_s , while \bar{M}_t is learned based on random initialization.

For each input x_i , the framework generates four outputs, namely the basal DNA z_i , the source model output y_i^s , and the homologous (non-homologous) target model output y_i^t (\bar{y}_i^t).

DNA assemble. After that, we combine the output of the DNA generator and the outputs of the source/target model to obtain a model DNA fragment based on each input x_i . The combination can be designed in various ways. In this paper, we assume the outputs are in the same dimension and fuse them by addition. For each input x_i , we can obtain three types of DNA fragments:

$$o_i^s \leftarrow z_i + y_i^s, \quad o_i^t \leftarrow z_i + y_i^t, \quad \bar{o}_i^t \leftarrow z_i + \bar{y}_i^t. \quad (4)$$

5.2 DNA similarity loss

In particular, the DNA similarity loss is designed to measure the similarity of two models' DNA in the latent space based on these representations. Inspired by Contrastive Learning [Chen et al., 2020], we consider a metric that ensures that the similarity of (o_i^s, o_i^t) in the latent space is not disclosed to (o_i^s, \bar{o}_i^t) . Note that our DNA similarity loss differs from previous contrastive losses since it further considers the relationships between the DNA fragments of the same model in a mini-batch of training data. To be specific, we not only preserve the relationships between (o_i^s, o_i^t) and (o_i^s, \bar{o}_i^t) based on a single input x_i , but also consider the intersection of information across the relations in \mathbb{O}_s , \mathbb{O}_t , and $\bar{\mathbb{O}}_t$. In other words, we involve more relationships in the loss function, as shown in Figure 3. The solid line represents the relationship used in previous works, while the dashed line represents the relationship between different DNA fragments within a model.

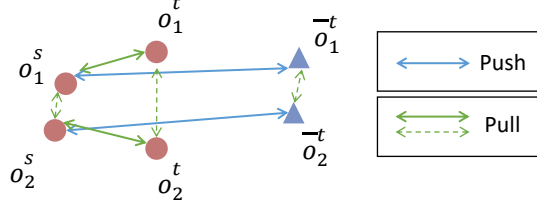


Figure 3: Similarity in DNA space .

Let $sim(u, v) = u^T v / \|u\| \|v\|$ denote the dot product between l_2 normalized vectors u and v (i.e. cosine similarity). We consider a training dataset of N examples and define a contrastive DNA generation loss on pairs of (o_i^s, o_i^t) and (o_i^s, \bar{o}_i^t) . The loss function is as follows:

$$\mathcal{L}_S = - \sum_{i=1}^N \log \frac{\exp(sim(o_i^s, o_i^t)/\tau)}{\sum_{k=1}^N \exp(sim(o_i^s, \bar{o}_k^t)/\tau)} \quad (5)$$

where τ denotes a temperature parameter [Chen et al., 2020].

We also consider the DNA distance in each model side as follows:

$$\mathcal{L}_I = - \sum_{i=1}^N \sum_{k=1}^{N-1} \log (\exp(sim(o_i^s, o_k^s)/\tau) + \exp(sim(o_i^t, o_k^t)/\tau) + \exp(sim(\bar{o}_i^t, \bar{o}_k^t)/\tau)), \quad i \neq k.$$

The DNA similarity loss is then computed using

$$\mathcal{L} = \mathcal{L}_S + \mathcal{L}_I + \lambda \|w_g\|_2 \quad (6)$$

where \mathcal{L}_S measures the difference between the DNA of the source model and the target model, \mathcal{L}_I measures the DNA from the same model. The last term is L_2 regularization on model parameters w_g of the DNA generator.

5.3 Provenance classifier

Finally, the outcome prediction network (i.e., a classifier) is employed to estimate the results of provenance prediction h' by taking DNA representations as input. Let $f_p(\cdot)$ denote the function learned by the outcome prediction network. We concatenate o_i^s and o_i^t (or o_i^s and \bar{o}_i^t) as input o_i^c . The loss function is as follows:

$$\mathcal{L}_{BCE} = - \frac{1}{N} \sum_{i=1}^N [h_i \log(h'_i) + (1 - h_i) \log(1 - h'_i)] \quad (7)$$

where h_i is the truth label² on each input o_i^c and $h'_i \leftarrow f_p(o_i^c)$.

5.4 Joint optimization

The DNA representation network and outcome prediction network are standard feed-forward neural networks with Dropout [Srivastava et al., 2014] and ReLU activation function. The overall loss function in Eq.(6) and (7) can be jointly optimized. Adam [Kingma and Ba, 2015] is adopted to solve the optimization problem.

5.5 Final prediction

In the final, our framework can make a prediction on different granularity of data, that is, we can set any models (e.g., M_1) in the target model part to verify if it is a homologous model with the source model M_s on DNA fragment o or DNA set \mathbb{O} . For the granularity of DNA fragment, we conduct the final provenance prediction as follows:

$$f(x_i, M_s, M_1) = \begin{cases} 1, & \text{if } f_p(o_i^c) \rightarrow 1 \\ 0, & \text{otherwise} \end{cases} \quad (8)$$

² $h = 1$ if M_s and M_t are homologous and 0 otherwise.

Table 1: Test accuracy of the proposed MGMP on CV task with and without (shown in parentheses) the DNA generator module.

Source		Model pool		Evaluation		Performance
Data	Model	Data	Model	Data	Model	Accuracy
CIFAR10	ResNet18	CIFAR100 (3 6 8 9 5)	ResNet18	CIFAR100 (1 2 4 7 0)	ResNet18	0.9193 (0.7529)
CIFAR10	ResNet18	CIFAR100 (6 7 0 1 2)	ResNet18	CIFAR100 (3 4 5 8 9)	ResNet18	0.9511 (0.8219)
CIFAR10	ResNet18	CIFAR100 (9 3 7 8 1)	ResNet18	CIFAR100 (4 2 5 0 6)	ResNet18	0.9607 (0.8030)
CIFAR10	ViT-small	CIFAR100 (3 6 8 9 5)	ViT-small	CIFAR100 (1 2 4 7 0)	ViT-small	0.9164 (0.8326)

where o_i^c is the concatenation of DNA fragment o_i^s and o_i^1 corresponding to x_i for $x_i \in D_s$. For the granularity of the model DNA set, we can compute the average results by considering the whole DNA fragments: $f(D_s, M_s, M_1) = 1$ if $\frac{1}{N} \sum_{i=1}^N f_p(o_i^c) \rightarrow 1$, and 0 otherwise³.

6 Experiments

To evaluate the effectiveness of our proposed framework, we conduct experiments on several commonly used benchmark datasets in CV and NLP. Specifically, we evaluate our framework on an image classification task using CIFAR-10 and CIFAR-100, as well as on a text classification task using the AGNews, YahooQA, and 20Newsgroups datasets, etc. The main experimental results are presented in the main paper, while additional results, e.g., parameter set/analysis, ablation experiment, and results with error bars, can be found in the supplemental material.

6.1 Experiments on CV benchmarks

Experimental setups. We first conduct the experiment on a common image classification task. An example is described as follows: As shown in the first row of Table 1, we initialize the model architecture as ResNet18 [He et al., 2016] and train the source model M_s on CIFAR10. Then, we employ CIFAR100 to construct model pools and evaluation datasets by partitioning it into 10 disjoint 10-way classification parts. We randomly choose 5 parts (e.g., 3 6 8 9 5) as data to train 10 models (5 homologous and 5 non-homologous) which are in the model pool and choose the rest to train multiple homologous/non-homologous models as evaluation data.

To gain deeper insights into how specific DNA fragments contribute to the overall prediction, we show performance on the granularity of the DNA fragment. Let N be the total number of training data of the source model and A_n (A_o) be the total number of data that can be identified correctly if we test the homologous (non-homologous) model as the target model. The test accuracy is defined as $Accuracy = \frac{A_n + A_o}{2N}$.

Experimental results. Table 1 presents the results of our proposed method under ResNet18 and ViT-small model structures on various datasets. Our method’s performance is consistently superior across all datasets, demonstrating its effectiveness in verifying the provenance of models. We compare the performance of our proposed method (MGMP) with and without the DNA generator module (Figure 2) and observe that the inclusion of the DNA generator improves the provenance prediction accuracy. To the best of our knowledge, there is no related method that has investigated the MP task. Specifically, the test accuracy obtained without the DNA generator (shown in parentheses) is lower, highlighting the importance of the DNA generator module in our proposed framework.

6.2 Experiments on NLP benchmarks

Experimental setups. We employ the DistilBERT architecture [Sanh et al., 2019] for text classification tasks on various benchmark NLP datasets, as reported in Table 2. Similar to our experimental setup for CV tasks, we randomly select one dataset to train the source model, and three datasets to form the model pool. For evaluation, we use two datasets to train homologous or non-homologous

³In practice, we can also employ a threshold δ for determining the final prediction, i.e., $\frac{1}{N} \sum_{i=1}^N f_p(o_i^c) \geq \delta$. and δ can be seen as a degree of similarity of DNA. The choice of threshold depends on the specific context and requirements of the problem at hand.

Table 2: Test accuracy of the proposed MGMP on NLP task with and without (shown in parentheses) the DNA generator module.

Source		Model pool		Evaluation		Performance
Data	Model	Data	Model	Data	Model	Accuracy
AGNews	DistilBERT	Amazon / DBPedia/YahooQA	DistilBERT	20Newsgroups/Yelp	DistilBERT	0.8377 (0.7203)
YahooQA	DistilBERT	20Newsgroup/DBPedia/Amazon	DistilBERT	AGNews/Yelp	DistilBERT	0.8625 (0.7875)
20Newsgroups	DistilBERT	YahooQA/Yelp/20Newsgroups	DistilBERT	AGNews/DBPedia	DistilBERT	0.9395 (0.8371)

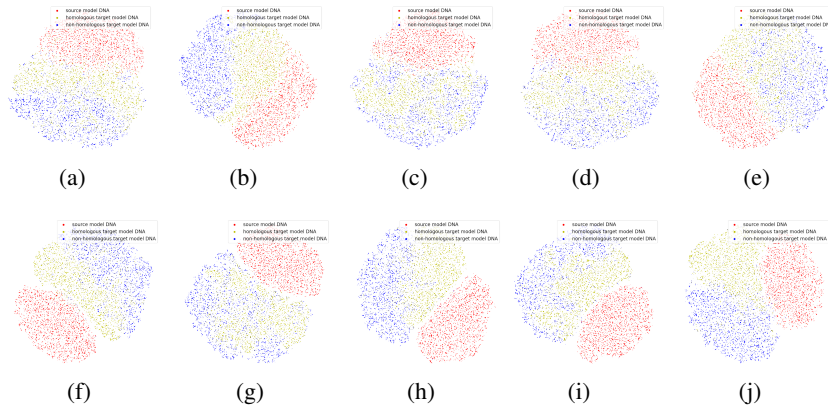


Figure 4: The visualization of the DNA fragments of the source model (red), homologous target model (yellow), and non-homologous target model (blue).

models. Due to space limitations, some experiments on larger models are provided in the supplemental material.

Experimental results. The results in Table 2 demonstrate that MGMP performs exceptionally well on the text classification task when applied to the DistilBERT model. Similarly, MGMP without the DNA generator achieves worse accuracy than the original MGMP. These results are consistent with previous evaluations on CV task. The consistent findings across both the text classification and computer vision tasks emphasize the robustness and generalizability of our approach.

6.3 Experimental visualization.

We visualize the generated DNA fragments of the first CV experiment (i.e., the first row of Table 1). Figure 4 shows T-SNE visualizations of the space of DNA fragments for each class data of CIFAR10. The red points represent the generated DNA of the source model, the yellow ones are DNA from homologous target models, and the blue ones are DNA from non-homologous target models. We observe that the points belonging to homologous models are almost much closer to each other than points from non-homologous models. Specifically, the distance between the red and yellow points is much smaller than the distance between the red and blue points. This suggests that our proposed framework is effective in capturing the similarity between homologous models and distinguishing them from non-homologous models.

7 Conclusion

In this paper, we present an efficient model representation learning framework for tackling an important problem, namely Model Provenance. We introduce a new idea of model DNA to represent a machine learning model. The proposed framework first constructs the model DNA space which preserves similarity information between homologous models and enhances the differences between non-homologous models, and then uses model DNA to obtain provenance outcomes. Experimental results on different tasks show that our method achieves good performance in the MP task.

References

- Mohammad Shehab, Laith Abualigah, Qusai Shambour, Muhannad A. Abu-Hashem, Moh'd Khaled Yousef Shambour, Ahmed Izzat Alsalibi, and Amir H. Gandomi. Machine learning in medical applications: A review of state-of-the-art methods. *Computers in Biology and Medicine*, 145:105458, 2022.
- Matthew F Dixon, Igor Halperin, and Paul Bilokon. *Machine learning in Finance*, volume 1170. Springer, 2020.
- Mingfu Xue, Yushu Zhang, Jian Wang, and Weiqiang Liu. Intellectual property protection for deep learning models: Taxonomy, methods, attacks, and evaluations. *IEEE Transactions on Artificial Intelligence*, 3(6):908–923, 2021.
- German Ignacio Parisi, Ronald Kemker, Jose L. Part, Christopher Kanan, and Stefan Wermter. Continual lifelong learning with neural networks: A review. *Neural Networks*, 113:54–71, 2019a.
- Sanket Vaibhav Mehta, Darshan Patil, Sarath Chandar, and Emma Strubell. An empirical investigation of the role of pre-training in lifelong learning. *CoRR*, abs/2112.09153, 2021.
- Mariya Toneva, Alessandro Sordoni, Remi Tachet des Combes, Adam Trischler, Yoshua Bengio, and Geoffrey J. Gordon. An empirical study of example forgetting during deep neural network learning. In *ICLR*, 2019.
- Matthias De Lange, Rahaf Aljundi, Marc Masana, Sarah Parisot, Xu Jia, Ales Leonardis, Gregory G. Slabaugh, and Tinne Tuytelaars. A continual learning survey: Defying forgetting in classification tasks. *IEEE transactions on pattern analysis and machine intelligence*, 44(7):3366–3385, 2022.
- Zhiyuan Chen and Bing Liu. *Lifelong Machine Learning, Second Edition*. Synthesis Lectures on Artificial Intelligence and Machine Learning. Morgan & Claypool Publishers, 2018.
- German I Parisi, Ronald Kemker, Jose L Part, Christopher Kanan, and Stefan Wermter. Continual lifelong learning with neural networks: A review. *Neural networks*, 113:54–71, 2019b.
- James Kirkpatrick, Razvan Pascanu, Neil Rabinowitz, Joel Veness, Guillaume Desjardins, Andrei A Rusu, Kieran Milan, John Quan, Tiago Ramalho, Agnieszka Grabska-Barwinska, et al. Overcoming catastrophic forgetting in neural networks. *Proceedings of the national academy of sciences*, 114(13):3521–3526, 2017.
- Friedemann Zenke, Ben Poole, and Surya Ganguli. Continual learning through synaptic intelligence. In *ICML*, pages 3987–3995, 2017.
- David Lopez-Paz and Marc' Aurelio Ranzato. Gradient episodic memory for continual learning. In *NIPS*, pages 6467–6476, 2017.
- Arslan Chaudhry, Marc' Aurelio Ranzato, Marcus Rohrbach, and Mohamed Elhoseiny. Efficient lifelong learning with A-GEM. In *ICLR*, 2019.
- Zirui Wang, Sanket Vaibhav Mehta, Barnabás Póczos, and Jaime G. Carbonell. Efficient meta lifelong-learning with limited memory. In *EMNLP*, pages 535–548, 2020.
- Andrei A. Rusu, Neil C. Rabinowitz, Guillaume Desjardins, Hubert Soyer, James Kirkpatrick, Koray Kavukcuoglu, Razvan Pascanu, and Raia Hadsell. Progressive neural networks. *CoRR*, abs/1606.04671, 2016.
- Rahaf Aljundi, Punarjay Chakravarty, and Tinne Tuytelaars. Expert gate: Lifelong learning with a network of experts. In *CVPR*, pages 7120–7129, 2017.
- Shagun Sodhani, Sarath Chandar, and Yoshua Bengio. Toward training recurrent neural networks for lifelong learning. *Neural Computing*, 32(1):1–35, 2020.
- Yoshua Bengio, Aaron C. Courville, and Pascal Vincent. Representation learning: A review and new perspectives. *IEEE Transactions on Pattern Analysis and Machine Intelligence.*, 35(8):1798–1828, 2013.

- Phuc H. Le-Khac, Graham Healy, and Alan F. Smeaton. Contrastive representation learning: A framework and review. *IEEE Access*, 8:193907–193934, 2020.
- Ting Chen, Simon Kornblith, Mohammad Norouzi, and Geoffrey E. Hinton. A simple framework for contrastive learning of visual representations. In *ICML*, pages 1597–1607, 2020.
- Aäron van den Oord, Yazhe Li, and Oriol Vinyals. Representation learning with contrastive predictive coding. *CoRR*, abs/1807.03748, 2018.
- Congzheng Song and Vitaly Shmatikov. Auditing data provenance in text-generation models. In *KDD*, pages 196–206, 2019.
- Xin Mu, Ming Pang, and Feida Zhu. Data provenance via differential auditing. *CoRR*, abs/2209.01538, 2022.
- Pratyush Maini, Mohammad Yaghini, and Nicolas Papernot. Dataset inference: Ownership resolution in machine learning. In *ICLR*, 2021.
- Reza Shokri, Marco Stronati, Congzheng Song, and Vitaly Shmatikov. Membership inference attacks against machine learning models. In *S&P*, pages 3–18, 2017.
- Hongsheng Hu, Zoran Salcic, Gillian Dobbie, and Xuyun Zhang. Membership inference attacks on machine learning: A survey. *CoRR*, abs/2103.07853, 2021.
- Seyed-Iman Mirzadeh, Mehrdad Farajtabar, Razvan Pascanu, and Hassan Ghasemzadeh. Understanding the role of training regimes in continual learning. In *NeurIPS*, 2020.
- Nitish Shirish Keskar, Dheevatsa Mudigere, Jorge Nocedal, Mikhail Smelyanskiy, and Ping Tak Peter Tang. On large-batch training for deep learning: Generalization gap and sharp minima. In *ICLR*, 2017.
- Mansheej Paul, Surya Ganguli, and Gintare Karolina Dziugaite. Deep learning on a data diet: Finding important examples early in training. In *NeurIPS*, pages 20596–20607, 2021.
- Kaiming He, Xiangyu Zhang, Shaoqing Ren, and Jian Sun. Deep residual learning for image recognition. In *CVPR*, pages 770–778, 2016.
- Alex Krizhevsky, Ilya Sutskever, and Geoffrey E. Hinton. Imagenet classification with deep convolutional neural networks. In *NIPS*, pages 1106–1114, 2012.
- Matt Ridley. Genome: the autobiography of a species in 23 chapters. *Nature Medicine*, 6(1):11–11, 2000.
- Ian J. Goodfellow, Jean Pouget-Abadie, Mehdi Mirza, Bing Xu, David Warde-Farley, Sherjil Ozair, Aaron C. Courville, and Yoshua Bengio. Generative adversarial networks. *Communications of the ACM*, 63(11):139–144, 2020.
- Nitish Srivastava, Geoffrey E. Hinton, Alex Krizhevsky, Ilya Sutskever, and Ruslan Salakhutdinov. Dropout: a simple way to prevent neural networks from overfitting. *The Journal of Machine Learning Research*, 15(1):1929–1958, 2014.
- Diederik P. Kingma and Jimmy Ba. Adam: A method for stochastic optimization. In Yoshua Bengio and Yann LeCun, editors, *ICLR*, 2015.
- Victor Sanh, Lysandre Debut, Julien Chaumond, and Thomas Wolf. Distilbert, a distilled version of BERT: smaller, faster, cheaper and lighter. *CoRR*, abs/1910.01108, 2019.

A Discussion

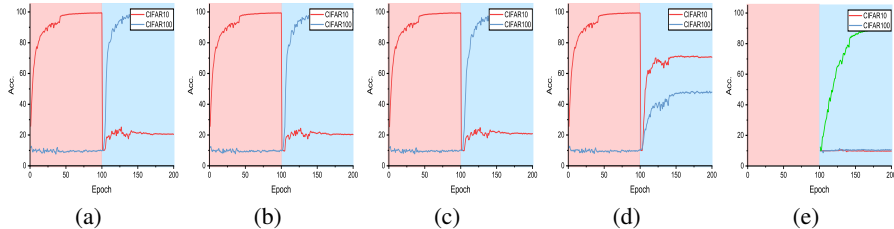


Figure 5: AlexNet. (a) No replace layer. (b) Replace target model’s last layer with source model. (c) Replace last two layers. (d) Replace last three layers. (e) Replace target model (random initialization)’s last three layers with source model.

In addition to the previous ResNet experiments in Section 3, we conducted another experiment on the model AlexNet, the results of which are presented in Figure 5. Remarkably, the findings from the AlexNet experiment align with the observations from the earlier experiments.

B Implementation Details

B.1 Datasets

The datasets used in this study are summarized in Table 3. This table provides essential information about each dataset, including the dataset name, a brief description, the number of samples, and the types of features contained in each dataset. To accommodate the computational requirements and ensure efficient experimentation, we sampled a subset (20,000) from some NLP datasets as the training data.

Table 3: Description of Datasets

Dataset Name	Description	Number of Samples	Features
CIFAR-10	A dataset of images for 10 categories	50,000	RGB (32×32)
CIFAR-100	A dataset of images for 100 categories	50,000	RGB (32×32)
AGNews	A dataset of news articles	20,000	Text (4 classes)
YahooQA	A dataset of questions and answers	20,000	Text (10 classes)
20 Newsgroups	A dataset of newsgroup documents	13,370	Text (20 classes)
DBPedia	A dataset of Wikipedia articles	20,000	Text (14 classes)
Amazon Reviews	A dataset of Amazon customer reviews	20,000	Text (5 classes)
Yelp Review	A dataset of Yelp reviews	20,000	Text (5 classes)

B.2 Experimental settings.

All experiments were conducted using Python programming language on a machine equipped with an Intel Core CPU, 64 GB of memory, and an NVIDIA Corporation GV100GL [Tesla V100 SXM2 32GB] GPU. We show the details of our proposed framework MGMP in Table 4. In the Computer Vision (CV) task, the generator’s structure is set using the ResNet50 architecture. ResNet50 is a popular Convolutional Neural Network (CNN) architecture commonly used for image classification tasks. It consists of 50 layers, including convolutional layers, pooling layers, and fully connected layers. The model parameters, such as the learning rate, are set to their default values. In the NLP task, the structure of the generator is set as DistilBERT, and the model parameters are also set to their default values.

Table 4: The details of MGMP

Task	Generator	$ z $	$ l $	Classifier
CV	ResNet50	10	20	three fully connected layers
NLP	DistilBERT	768	1536	three fully connected layers

B.3 Full results of CV task.

Table 5 presents additional experimental results with corresponding standard deviation computed over 5 runs, respectively, for the CV and NLP task. In this set of experiments, we evaluate a different model structure AlexNet, and the experimental results are consistent with the main paper.

Table 5: Test accuracy of the proposed MGMP on CV task with and without (shown in parentheses) the DNA generator module.

Source		Model pool		Evaluation		Performance
Data	Model	Data	Model	Data	Model	Accuracy
CIFAR10	ResNet18	CIFAR100 (3 6 8 9 5)	ResNet18	CIFAR100 (1 2 4 7 0)	ResNet18	0.9193± 0.0232 (0.7529±0.0347)
CIFAR10	ResNet18	CIFAR100 (6 7 0 1 2)	ResNet18	CIFAR100 (3 4 5 8 9)	ResNet18	0.9511± 0.0432 (0.8219±0.0332)
CIFAR10	ResNet18	CIFAR100 (9 3 7 8 1)	ResNet18	CIFAR100 (4 2 5 0 6)	ResNet18	0.9607± 0.0483 (0.8030± 0.0451)
CIFAR10	AlexNet	CIFAR100 (3 6 8 9 5)	AlexNet	CIFAR100 (1 2 4 7 0)	AlexNet	0.9025± 0.0472 (0.7220±0.0687)
CIFAR10	AlexNet	CIFAR100 (6 7 0 1 2)	AlexNet	CIFAR100 (3 4 5 8 9)	AlexNet	0.9247± 0.0392 (0.8471±0.0417)
CIFAR10	AlexNet	CIFAR100 (9 3 7 8 1)	AlexNet	CIFAR100 (4 2 5 0 6)	AlexNet	0.9106± 0.0331 (0.8231± 0.0442)
CIFAR10	ViT-small	CIFAR100 (3 6 8 9 5)	ViT-small	CIFAR100 (1 2 4 7 0)	ViT-small	0.9164±0.0224 (0.8326±0.0306)

B.4 Full results of NLP task.

Table 6 presents additional experimental results on the BERT based model. The experimental results are consistent with the main paper.

Table 6: Test accuracy of the proposed MGMP on NLP task with and without (shown in parentheses) the DNA generator module.

Source		Model pool		Evaluation		Performance
Data	Model	Data	Model	Data	Model	Accuracy
AGNews	DistilBERT	Amazon / DBPedia/YahooQA	DistilBERT	20Newsgroups/Yelp	DistilBERT	0.8377±0.0778 (0.7203±0.0936)
YahooQA	DistilBERT	20Newsgroup/DBPedia/Amazon	DistilBERT	AGNews/Yelp	DistilBERT	0.8625±0.0903 (0.7875±0.1003)
20Newsgroups	DistilBERT	YahooQA/Yelp/20Newsgroups	DistilBERT	AGNews/DBPedia	DistilBERT	0.9395±0.0554 (0.8371±0.0964)
AGNews	BERT-base	Amazon / DBPedia/YahooQA	BERT-base	20Newsgroup/Yelp	BERT-base	0.8656 ±0.0802 (0.7074±0.0918)

B.5 The analysis of MGMP

The analysis of the MGMP framework aims to gain a comprehensive understanding of the individual components and processes within the approach. In this study, we specifically investigate the influence of different generator structures and various methods of DNA assembly. To isolate the effects of these factors, we conduct separate evaluations where one component is varied while keeping other components fixed. To establish a baseline experimental set, we consider the first row of Table 2 as the initial configuration.

We observed that the performance of different generator structures remained consistent across various evaluation metrics. We found that the DNA assembly process had a notable effect on the results. Different ways of assembling the DNA fragments resulted in variations in performance. Our results indicate that increasing the dimensionality of the DNA representation can lead to improved results within the MGMP framework. By incorporating additional dimensions into the DNA, we can capture more nuanced information and potentially enhance the performance of the model. By analyzing the results in Table 7, we gain insights into the contributions of individual components and their interactions within the MGMP framework. This analysis helps us identify the optimal configuration and provides valuable guidance for future improvements and refinements of the approach.

B.6 The experimental visualization on NLP task.

In addition to the previous visualization on CV task, we also provide visualization on NLP task in Figure 6. We visualize the generated DNA fragments of the third NLP experiment (i.e., the third row of Table 2).

Table 7: Components analysis: Test accuracy of MGMP with various DNA generator structures.

Component		Performance
Generator	DNA assemble ($ o $)	Accuracy
ResNet50	addition (10)	0.9193
ViT-samll	addition (10)	0.9004
ViT-base	addition (10)	0.9137
ResNet50	concatenate (20)	0.9264
ResNet50	concatenate (60)	0.9416
ResNet50	concatenate (110)	0.9478

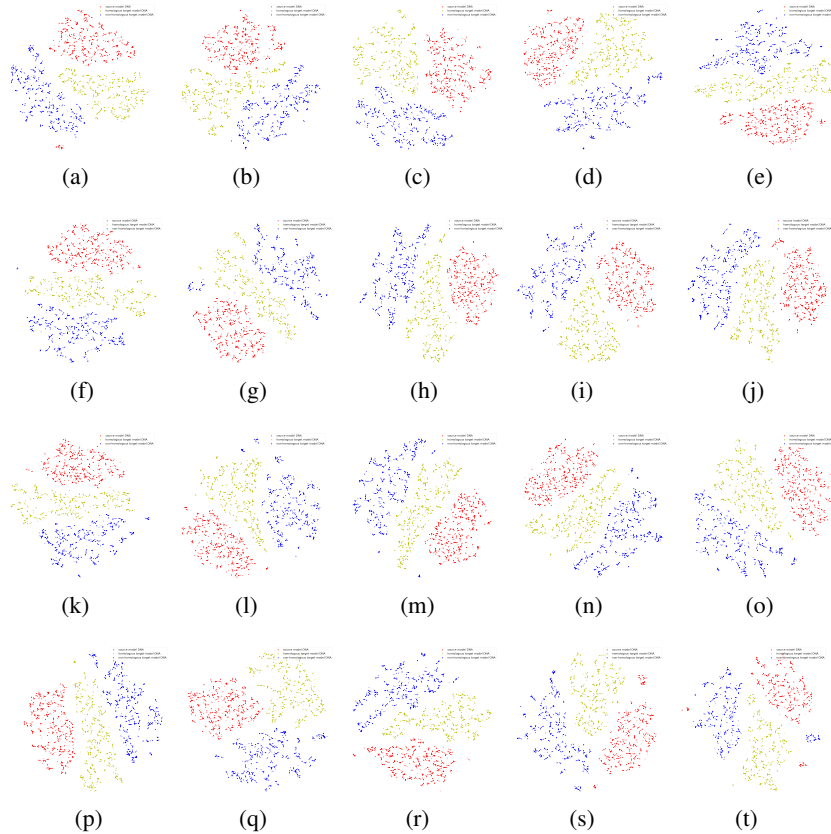


Figure 6: The visualization of the DNA fragments of the source model (red), homologous target model (yellow), and non-homologous target model (blue).